

Carbamoyl Phosphate Synthetase: Caught in the Act of Glutamine Hydrolysis^{†,‡}James B. Thoden,[§] Sophie G. Miran,^{||} James C. Phillips,[⊥] Andrew J. Howard,[#] Frank M. Raushel,^{||} and Hazel M. Holden^{*§}

Institute for Enzyme Research, The Graduate School, and Department of Biochemistry, College of Agricultural and Life Sciences, University of Wisconsin—Madison, 1710 University Avenue, Madison, Wisconsin 53705, Department of Chemistry, Texas A&M University, College Station, Texas 77843, Bruker AXS Inc., 6300 Enterprise Lane, Madison, Wisconsin 53719, and Center for Synchrotron Radiation Research and Instrumentation, Department of Biological, Chemical, and Physical Sciences, Illinois Institute of Technology, 3101 South Dearborn Street, Chicago, Illinois 60616

Received April 7, 1998; Revised Manuscript Received May 5, 1998

ABSTRACT: Carbamoyl phosphate synthetase from *Escherichia coli* catalyzes the production of carbamoyl phosphate from two molecules of $Mg^{2+}ATP$, one molecule of bicarbonate, and one molecule of glutamine. The enzyme consists of two polypeptide chains referred to as the large and small subunits. While the large subunit provides the active site responsible for the binding of nucleotides and other effector ligands, the small subunit contains those amino acid residues that catalyze the hydrolysis of glutamine to glutamate and ammonia. From both amino acid sequence analyses and structural studies it is now known that the small subunit belongs to the class I amidotransferase family of enzymes. Numerous biochemical studies have suggested that the reaction mechanism of the small subunit proceeds through the formation of the glutamyl thioester intermediate and that both Cys 269 and His 353 are critical for catalysis. Here we describe the X-ray crystallographic structure of carbamoyl phosphate synthetase from *E. coli* in which His 353 has been replaced with an asparagine residue. Crystals employed in the investigation were grown in the presence of glutamine, and the model has been refined to a crystallographic *R*-factor of 19.1% for all measured X-ray data from 30 to 1.8 Å resolution. The active site of the small subunit clearly contains a covalently bound thioester intermediate at Cys 269, and indeed, this investigation provides the first direct structural observation of an enzyme intermediate in the amidotransferase family.

Carbamoyl phosphate synthetase from *Escherichia coli*, hereafter referred to as CPS, catalyzes the formation of carbamoyl phosphate which is subsequently employed in both arginine and pyrimidine biosynthesis in eukaryotes and prokaryotes and in the urea cycle in most terrestrial vertebrates. Quite remarkably, CPS produces carbamoyl phosphate from two molecules of $Mg^{2+}ATP$, one molecule of bicarbonate, and one molecule of glutamine. The molecular architecture of the enzyme from *E. coli*, now known to 2.1 Å resolution (1, 2), is displayed in Figure 1. As can be seen, the enzyme consists of a large subunit responsible for binding the two molecules of $Mg^{2+}ATP$ and a small subunit perched at the top of this larger polypeptide chain.

As expected from its biochemical role, CPS is a member of the glutamine amidotransferase class of enzymes. These proteins specifically function by employing glutamine as a

direct source of ammonia for the subsequent biosynthesis of nitrogen-containing intermediates. On the basis of primary amino acid sequence comparisons, two classes of glutamine amidotransferases have been identified thus far. The TrpG-type or class I family includes CPS, anthranilate synthase, GMP synthetase, CTP synthetase, and aminodeoxychorismate synthase, among others, while the PurF-type or class II family contains enzymes such as glutamine 5-phosphoribosyl-1-pyrophosphate amidotransferase, glucosamine 6-phosphate synthase, glutamate synthase, and asparagine synthetase (3). In CPS from *E. coli*, the small subunit, encoded by the *carA* gene, contains the amidotransferase domain of this enzyme (4, 5). As in the small subunit of CPS, the active sites of all glutamine amidotransferases contain a critical cysteine residue thought to initiate a nucleophilic attack at the amide functional group of the glutamine substrates. In CPS and GMP synthetase, for which high-resolution X-ray structures are known (1, 2, 6), this active site nucleophile adopts dihedral angles of approximately $\phi = 60^\circ$ and $\psi = -96^\circ$, a characteristic feature of those enzymes belonging to the so-called α/β hydrolase fold (7).

In CPS from *E. coli*, this active site thiol group has been identified as Cys 269 on the basis of both chemical modification experiments and subsequent site-directed mutagenesis analyses (8, 9, 10, 11). In addition, both site-directed mutagenesis experiments and amino acid sequence

[†] This research was supported in part by grants from the NIH (GM55513 to H.M.H. and DK30343 to F.M.R.) and the NSF (BIR-9317398 shared instrumentation grant).

[‡] X-ray coordinates have been deposited in the Brookhaven Protein Data Bank (entry 1A9X) and will be released upon publication.

* To whom correspondence should be addressed.

[§] University of Wisconsin—Madison.

^{||} Texas A&M University.

[⊥] Bruker AXS Inc.

[#] Illinois Institute of Technology.

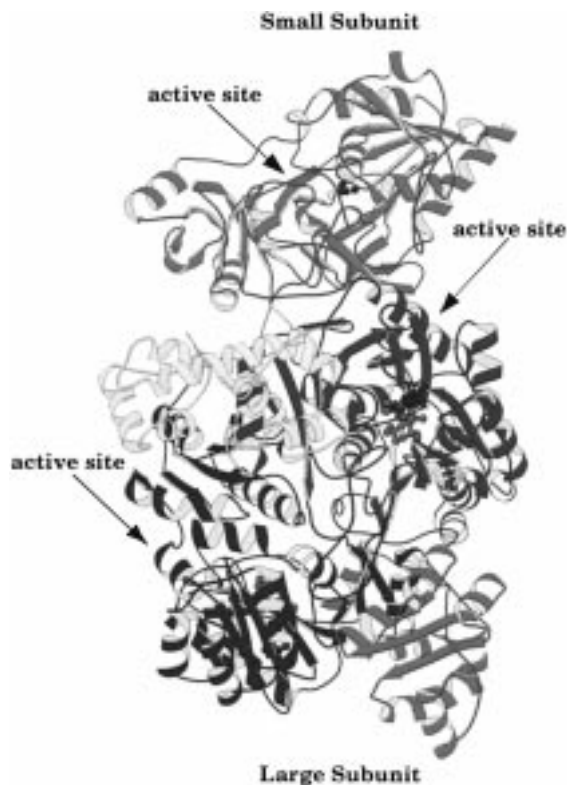


FIGURE 1: Ribbon representation of the CPS α,β -heterodimer. The small subunit, or amidotransferase component of CPS, is displayed in magenta. In the large subunit, the polypeptide chain regions defined by Met 1–Glu 403, Val 404–Ala 553, Asn 554–Asn 936, and Ser 937–Lys 1073 are depicted in green, yellow, blue, and red, respectively. The active site cysteine in the small subunit (Cys 269) and the two ADP molecules bound in the large subunit are shown as ball-and-stick representations. The locations of the three active sites are indicated by the arrows. Note that the active site in the small subunit is separated from the first active site in the large subunit by approximately 45 Å and the two active sites of the large subunit are separated by approximately 35 Å. This ribbon representation is based on the model of Thoden (2).

alignments have revealed the presence of two histidine residues thought to play important roles in the proper functioning of Cys 269. Indeed, the replacement of His 353 with an asparagine residue has demonstrated that the imidazole ring of its side chain most likely serves to activate Cys 269 via general acid/base effects while substitution of His 312 for asparagine increases the K_m for glutamine considerably, thus suggesting that this residue participates in substrate binding (12). In agreement with these biochemical results, the recent three-dimensional structural investigation of CPS has demonstrated that $N^{\epsilon 2}$ of His 353 is located at 4.0 Å from S^{γ} of Cys 269 and that the carboxylate side chain of Glu 355 is within hydrogen-bonding distance to $N^{\delta 1}$ of His 353 (1, 2). Likewise, the high-resolution X-ray model of CPS has shown that His 312 is located in a position consistent with a role in substrate binding although in the original X-ray analysis the active site was not occupied by glutamine or any type of substrate analogue.

In light of the remarkable finding from the first X-ray investigation of CPS that the three active sites within the α,β -heterodimer are separated by nearly 100 Å, it was postulated that the ammonia derived from the hydrolysis of glutamine in the small subunit must be transferred to the first active site in the large subunit by some type of molecular

tunnel (1). The present working model for the generation of this ammonia within the amidotransferase domain or small subunit of CPS is illustrated in Scheme 1 (12).

As indicated, the carbonyl carbon of the glutamine side-chain carboxamide group is attacked by the thiolate anion of Cys 269, yielding a tetrahedral intermediate. The collapse of this intermediate is facilitated by protonation of the amino group by His 353, thereby forming a thioester intermediate and ammonia. The ammonia departs, after which the thioester intermediate is hydrolyzed presumably by a water molecule that has been activated through its interaction with His 353. Experimental support for such a glutamyl thioester intermediate in the reaction mechanism has been provided by the experiments of Lusty (13). In her biochemical analyses she was able to acid precipitate an apparently covalent complex between glutamine and CPS with the native protein but not with protein in which Cys 269 had been changed to a serine residue.

Here we provide unambiguous molecular evidence for the existence of a thioester intermediate in the reaction pathway of the CPS small subunit. The intermediate was trapped by the cocrystallization of glutamine with a form of CPS in which His 353 had been converted, via site-directed mutagenesis, to an asparagine residue. The absence of the imidazole moiety of His 353 significantly slowed the rate of hydrolysis of the thioester species in the crystalline lattice such that it was possible to observe the intermediate in the electron density map. The results describe here provide the first structural evidence for such an intermediate in the amidotransferase family.

MATERIALS AND METHODS

Purification and Crystallization Procedures. Protein employed in this investigation was purified as described elsewhere (12). Crystals were grown by batch at 4 °C as previously reported with the addition of 2.5 mM BeF_3 and 5 mM glutamine (1, 14). These crystals were stabilized with a synthetic mother liquor containing 1.0 M tetraethylammonium chloride, 8% (w/v) poly(ethylene glycol) 8000, 150 mM KCl, 2.5 mM ornithine, 2.5 mM MnCl_2 , 5 mM ADP, 5 mM glutamine, and 25 mM HEPES (pH 7.4). Following equilibration, the crystals were rapidly transferred to a cryoprotectant solution containing 1.4 tetraethylammonium chloride, 8% (w/v) poly(ethylene glycol) 8000, 250 mM KCl, 2.5 mM ornithine, 2.5 mM MnCl_2 , 5 mM ADP, 5 mM glutamine, 7.5% (v/v) ethylene glycol, and 25 mM HEPES (pH 7.4). They were then suspended in a thin film of the cryoprotectant solution in a loop of 20 μm surgical thread. The crystals were flash-cooled to -150 °C in a stream of nitrogen gas. These crystals belonged to the space group $P2_12_12_1$ with unit cell dimensions of $a = 152.1$ Å, $b = 164.4$ Å, and $c = 332.3$ Å and one α,β -heterotetramer per asymmetric unit.

X-ray Data Collection and Processing. The X-ray data employed for the least-squares model refinement described here were collected at the Advanced Photon Source on the Industrial Macromolecular Crystallography Association (IMCA-CAT) beamline 17-ID with a Bruker Mosaic CCD detector. These data were collected with 0.25° frames at a crystal-to-detector distance of 20 cm and the detector operated in unbinned (1024 \times 1024) mode with a 2θ value

Scheme 1

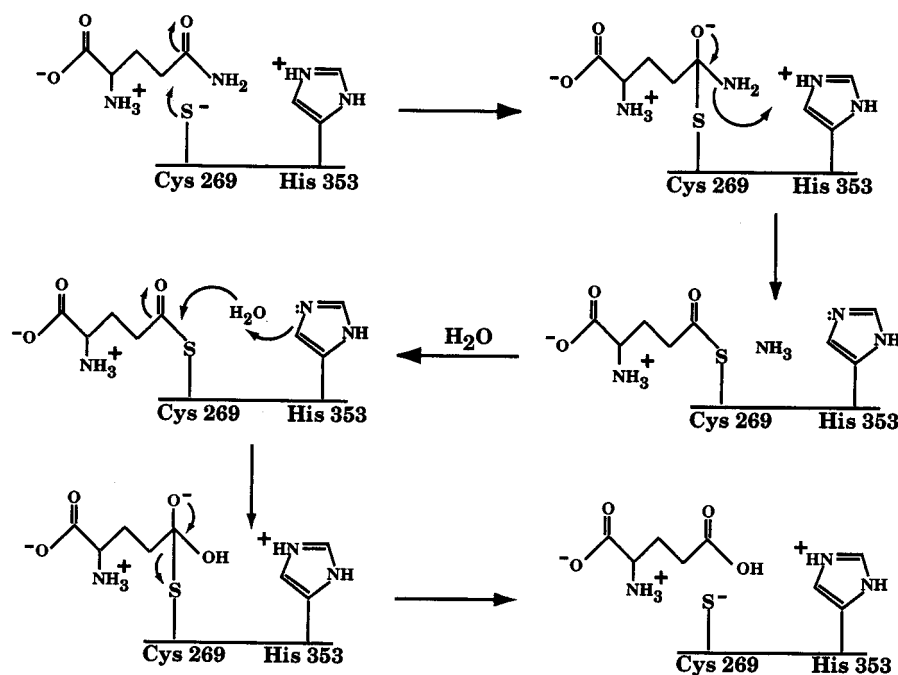


Table 1: Intensity Statistics

| | resolution range (Å) | | | | | | | | |
|-----------------------------------|----------------------|----------|--------|--------|--------|--------|--------|--------|--------|
| | overall | 30.0–3.6 | 2.86 | 2.50 | 2.27 | 2.11 | 1.98 | 1.88 | 1.80 |
| no. of measurements | 1676492 | 235090 | 245070 | 243030 | 228449 | 199064 | 180633 | 174371 | 170785 |
| no. of independent reflections | 700998 | 96723 | 93248 | 90417 | 86838 | 83239 | 80870 | 83775 | 85888 |
| % completeness | 92 | 99 | 97 | 95 | 92 | 87 | 86 | 88 | 91 |
| av <i>I</i> /av $\sigma(I)$ | 23.8 | 140 | 41.2 | 17.0 | 10.0 | 6.63 | 4.69 | 4.00 | 4.03 |
| <i>R</i> -factor ^a (%) | 6.5 | 2.8 | 4.8 | 9.9 | 11.7 | 15.9 | 20.8 | 23.9 | 27.5 |

^a *R*-factor = $(\sum |I - \bar{I}| / \sum I) \times 100$.

of +20. A complete X-ray data set was collected from a single crystal via three ω scans resulting in a total of 600 frames. Each frame required an exposure time of 10 s. While the crystal displayed X-ray diffraction to a nominal resolution of 1.6 Å, the radiation damage was severe enough beyond 1.8 Å resolution to render these data unusable for subsequent model refinement.

The frames were processed with SAINT2K (Bruker) and scaled with XCALIBRE (written by Drs. Gary Wesenberg and Ivan Rayment). From the 600 frames, 1 676 492 reflections were integrated which reduced to 700 998 unique reflections after scaling. Relevant X-ray data collection statistics can be found in Table 1.

Due to the large changes in the unit cell parameters upon flash-cooling, the structure reported here was necessarily “resolved” by molecular replacement (15) with the software package AMORE (16) and employing as a search model the complete tetrameric form of CPS previously determined at 2.1 Å resolution (2). Following rigid-body refinement, the model was subjected to least-squares analysis at 1.8 Å resolution with the software package TNT (17). After 15 cycles of refinement, the *R*-factor decreased from 38.9% to 31.8%. With over 5800 amino acid residues in the asymmetric unit, the goal of the model building process was to lower the *R*-factor as much as possible using an “averaged” α,β -heterodimer before finally rebuilding the entire tetramer in the asymmetric unit. Consequently, to expedite the

refinement and rebuilding processes, the electron densities corresponding to the four α,β -heterodimers in the asymmetric unit were averaged according to the algorithm of Bricogne (18), and one α,β -heterodimer and approximately 700 solvent molecules were rebuilt into the averaged map. Following this rebuilding process, the entire tetramer was reconstructed from the averaged α,β -heterodimer and placed back into the unit cell. Additional cycles of least-squares refinement decreased the *R*-factor to 21.5%. At this point the entire tetrameric model was adjusted in the asymmetric unit and additional solvent molecules were added. After 10 more cycles of refinement, the *R*-factor was reduced to 19.1% for all X-ray data between 30.0 and 1.8 Å and with root-mean-square deviations from “ideal” geometry of 0.014 Å for bond lengths, 2.5° for bond angles, and 0.10 Å for groups of atoms expected to be coplanar. The final model includes 8 ADP molecules, 12 manganese ions, 4 ornithines, 15 inorganic phosphates, 32 potassium ions, 28 chloride ions, 4528 water molecules, and 4 tetraethylammonium ions. The following side chains were modeled as multiple conformations: Arg 490, Asp 518, Asn 554, Met 772, Gln 821, Leu 947, Glu 1009, and Ser 1674 in α,β -heterodimer I, Arg 514, Arg 811, Glu 876, Lys 966, Arg 1004, Asn 1007, and Glu 1009 in α,β -heterodimer II, Asp 758, Glu 1009, Asn 1606, Glu 1645, and Met 1786 in α,β -heterodimer III, and Asp 6 in α,β -heterodimer IV. As shown in Figure 2, the only residues adopting dihedral angles well outside of the allowed regions

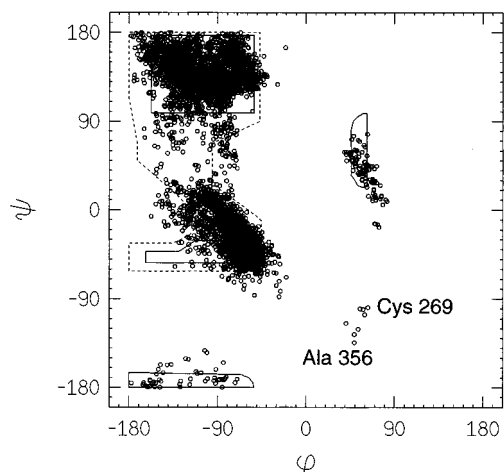


FIGURE 2: Ramachandran plot of all non-glycinyl main-chain dihedral angles. Fully allowed ϕ, ψ values are enclosed by solid lines; those partially allowed are enclosed by dashed lines.

of the Ramachandran plot are Cys 269 and Ala 356, both of which are located in the active site of the small subunit.

RESULTS AND DISCUSSION

The original goal in the crystallization of the site-directed mutant protein described here (namely, H353N) was to explore the mode of binding of glutamine in the CPS small subunit active site pocket. Indeed, from previous biochemical studies it was known that the replacement of this histidine with an asparagine residue resulted in a form of CPS unable to utilize glutamine as a substrate (12). Strikingly, however, the H353N mutant was still shown to bind glutamine as judged by the observation that the addition of this amino acid caused an enhancement of the bicarbonate-dependent ATPase reaction catalyzed by the large subunit of CPS. Shown in Figure 3 is a portion of the electron density map corresponding to Glu 355, His 353, and Cys 269 in the small

subunit of α, β -heterodimer I. For the sake of simplicity the following discussion will refer only to heterodimer I unless otherwise indicated. As can be seen, the electron density map is unambiguous and quite surprisingly demonstrates that the glutamyl thioester intermediate, rather than glutamine, is observed. This type of intermediate entrapment is not common but, indeed, has been reported, for example, in the X-ray crystallographic study of porcine pancreatic elastase (19) and in the recently described structural analysis of adenylosuccinate synthetase from *E. coli* (20). To our knowledge, however, the model reported here represents the first structural evidence for a glutamyl thioester intermediate in the amidotransferase family of proteins. The electron densities corresponding to the other three copies of the glutamyl thioester intermediate in the asymmetric unit are of quality equal to that shown in Figure 3 for α, β -heterodimer I. As a point of comparison, the average temperature factors for the four glutamyl intermediate moieties in the asymmetric unit are 32.5, 27.5, 26.9, and 31.5 Å^2 , respectively.

A close-up view of the small subunit active site is presented in Figure 4a. As expected, the binding pocket is fairly hydrophilic with a number of ordered water molecules surrounding the glutamyl thioester intermediate. From a previous study it was suggested that His 312 plays a role in substrate binding since replacement of this amino acid residue with an asparagine increased the K_m for glutamine from 105 μM to 20 mM in the full biosynthetic CPS reaction (12). Indeed, His 312 participates in the formation of the active site, but quite unexpectedly its side-chain imidazole group points away from the binding pocket. In addition, there are no direct electrostatic interactions between the glutamyl thioester intermediate and His 312. The manner in which the replacement of this histidine with an asparagine so dramatically affects the K_m of the small subunit for glutamine can only be addressed by additional structural analyses which are presently underway.

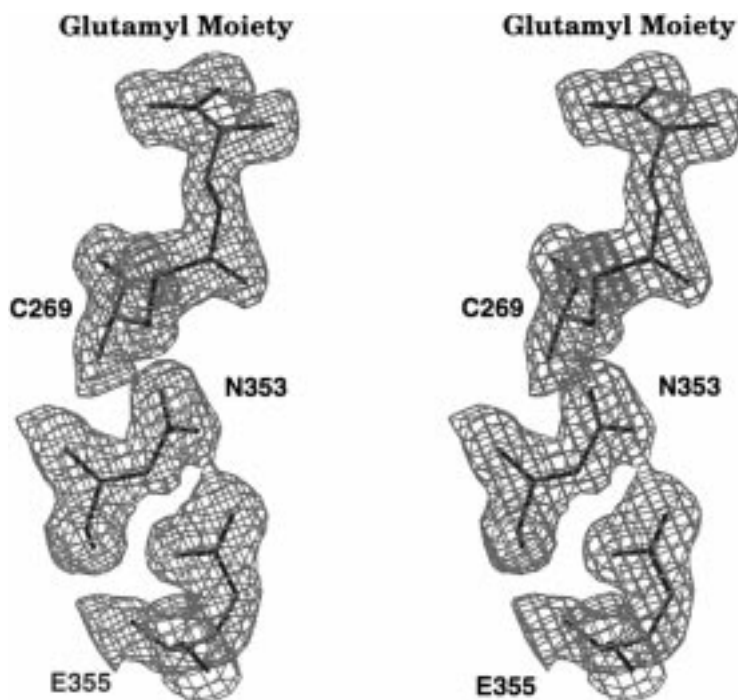
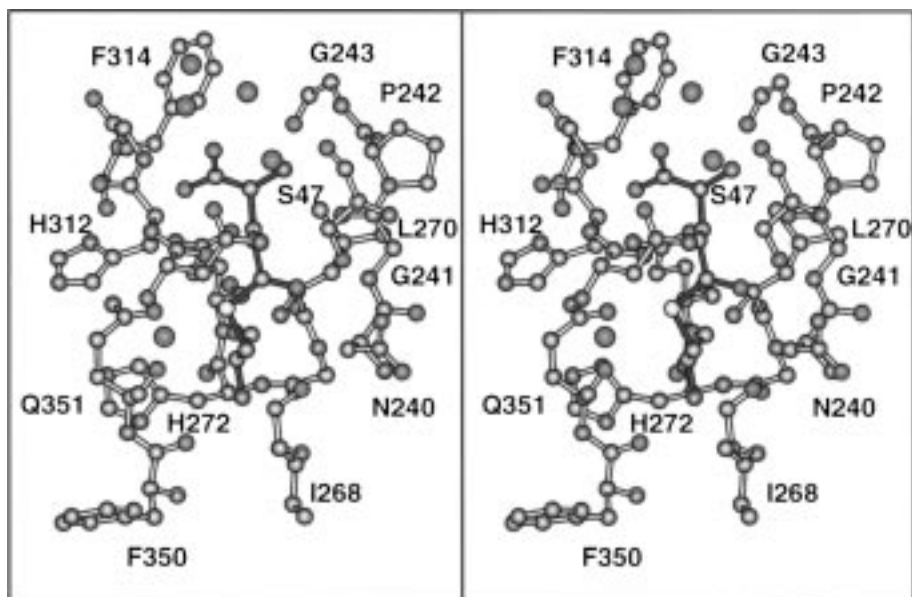
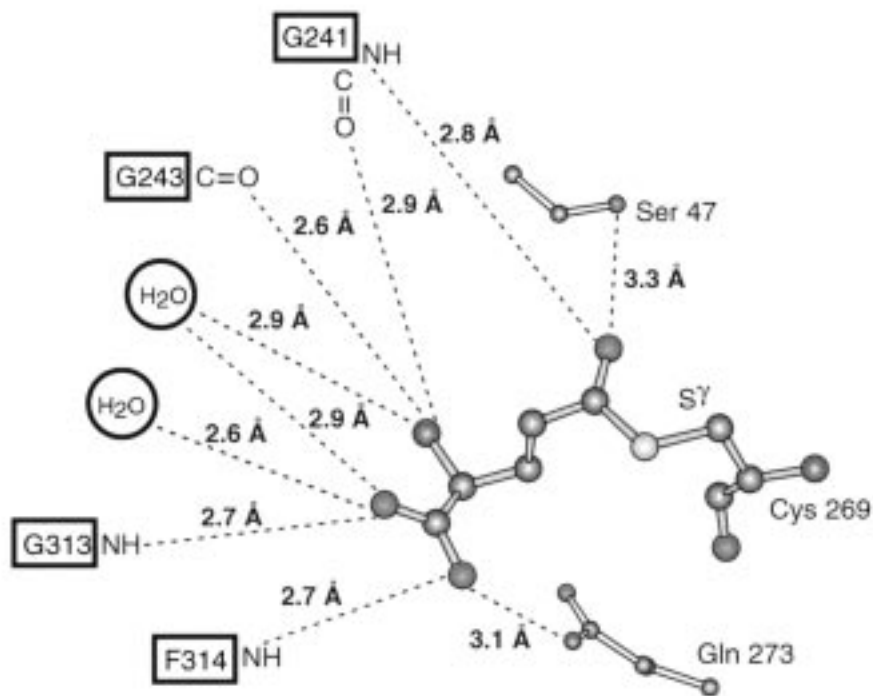


FIGURE 3: Electron density corresponding to the observed glutamyl thioester intermediate formed at Cys 269. The electron densities for Asn 353 and Glu 355 are also displayed. The map was contoured at 1σ and calculated with coefficients of the form $(2F_o - F_c)$.



(a)



(b)

FIGURE 4: Close-up view of the small subunit active site. (a) The region of the polypeptide chain, within approximately 4.0 Å of the glutamyl thioester intermediate, is shown. Ordered water molecules are indicated by the red spheres. (b) A cartoon diagramming potential electrostatic interactions between the intermediate and the protein is given.

The reaction mechanism of the small subunit of CPS, and presumably that of other members of the class I amidotransferase family, is thought to proceed via a tetrahedral intermediate as indicated in Scheme 1. From the cartoon of the hydrogen-bonding interactions between the glutamyl thioester intermediate and the protein given in Figure 4b, it can be speculated that O γ of Ser 47 and the backbone amide hydro-

gen of Gly 241 serve both to position the carbonyl carbon of the glutamine carboxamide group for nucleophilic attack by the thiolate of Cys 269 and to stabilize the developing oxyanion. In addition to these above-mentioned interactions, there are also numerous backbone carbonyl groups and amide hydrogens that serve to position the glutamyl thioester intermediate within the small subunit active site as indicated

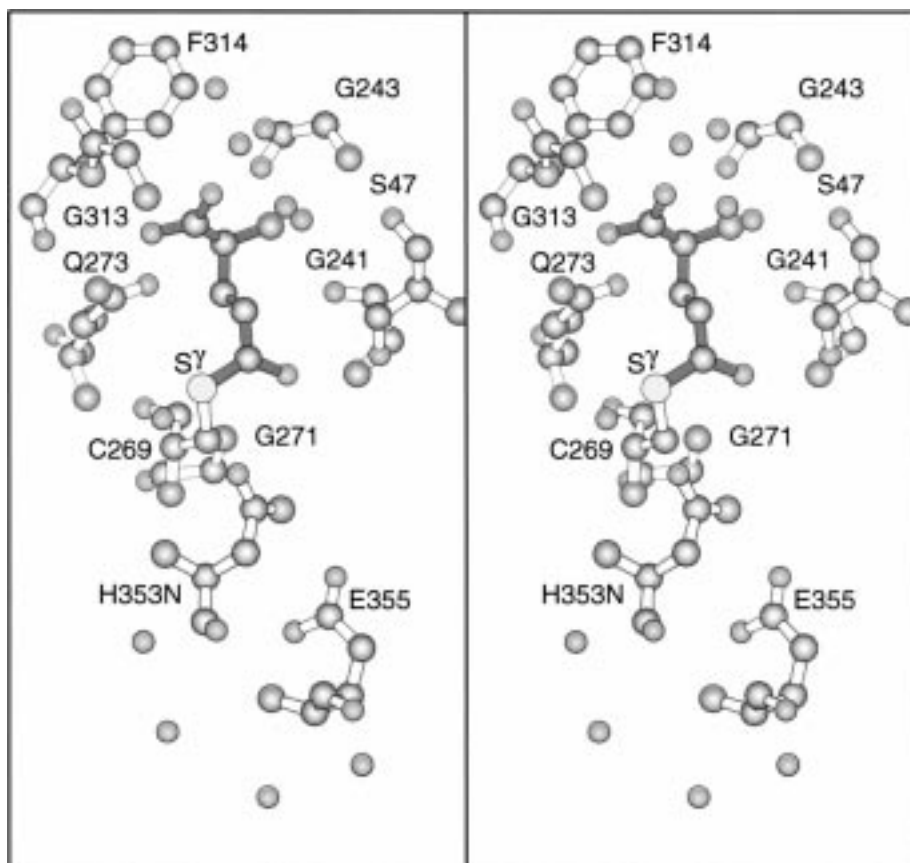


FIGURE 5: Orientation of the putative catalytic triad in the small subunit of CPS. Shown in stereo are the relative positions of Glu 355, Asn 353 (which in the native protein is a histidine residue), and Cys 269. Ordered water molecules are indicated by the red spheres. The overall role of Glu 355 in the catalytic mechanism is still unknown.

in Figure 4b. Besides Ser 47, the only other specific side-chain group interacting with the glutamyl thioester intermediate is that of Gln 273. The average bond distance between S^{γ} of Cys 269 and C^{δ} of the glutamyl moiety for the four molecules in the asymmetric unit is 1.71 Å. During the course of the least-squares refinement, this bond distance was restrained to 1.75 Å. A search of the Cambridge Data Base reveals that the typical carbon–sulfur bond distances in such thioesters range from 1.74 to 1.78 Å.

One immediate question concerns the manner in which the glutamyl thioester intermediate in this site-directed mutant protein is stable to hydrolysis. Certainly, the initial kinetic analyses of this H353N site-directed mutant protein did not indicate the formation of such an intermediate (12). Rather, all the biochemical data indicated that the glutaminase activity in this mutant enzyme was lost but the affinity of the small subunit for glutamine was not reduced since the activation constant for glutamine in the ATPase reaction ($54 \mu\text{M}$) was smaller than the Michaelis constant for glutamine ($K_m = 105 \mu\text{M}$) with the wild-type enzyme (12). The arrangement of the catalytic residues in the CPS small subunit is shown in Figure 5, and as can be seen, Glu 355, H353N, and Cys 269 are in the proper orientation for the formation of a “catalytic triad”, as suggested to occur in GMP synthetase (6). There is some discussion regarding the role of Glu 355, however. Whether there is any proton transfer between Glu 355 and His 353 in the native CPS molecule or rather whether the role of the glutamate is simply in the proper positioning of the imidazole side chain of the histidine is still open to question. Indeed, a site-directed mutagenesis

study on the glutaminase subunit of *p*-aminobenzoate synthetase has shown that replacement of the active site cysteine or histidine residue results in significant losses of enzymatic activity (21). On the other hand, when the putative catalytic triad was replaced with an alanine or aspartate, very little activity was lost, indeed, calling into the question the need for proton transfer between the glutamate and histidine moieties in the amidotransferases. Regardless of the role of Glu 355, perhaps the simplest explanation of the results presented here is that the small degree of ionization of Cys 269 was sufficient to permit attack as the thiolate on the carboxamide side-chain group of the glutamine bound in the active site to form the covalently bound intermediate. For the subsequent hydrolysis step to occur, however, a water molecule has to be activated, via some type of protein interaction, to carry out a nucleophilic attack at the carbonyl carbon of the thioester intermediate. By replacing His 353 with an asparagine, the activation of the hydrolytic water molecule would be significantly decreased. Since the thioester intermediate is formed with such high occupancy in the crystals of the H353N mutant, it appears that the rate of hydrolysis of this intermediate has been diminished to a greater extent than the rate of its formation. In addition, the X-ray data were collected at $-150 \text{ }^{\circ}\text{C}$, which would further reduce the catalytic rate of the enzyme.

A second important question that can be asked regards the structural changes that occur in both the large and small subunits of CPS upon formation of the glutamyl thioester intermediate. In fact, the structural changes are minimal such

that the α -carbons for the model reported here and those for the original CPS model superimpose with a root-mean-square deviation of 0.42 Å. As a further indication of the similarity between the two models, it should be noted that all backbone atoms for the small subunits with and without the bound intermediate superimpose with a root-mean-square deviation of 0.26 Å. Clearly, the lack of structural change between the two forms of CPS is in keeping with the fact that the buried surface area between the large and small subunits is over 2100 Å² with at least 35 specific hydrogen bonds between protein atoms from the two polypeptide chains (2).

In summary, the reaction mechanism for glutamine hydrolysis by the small subunit of CPS includes the binding of the substrate, the formation of a tetrahedral intermediate which collapses to form a covalently bound glutamyl thioester intermediate, hydrolysis of this intermediate by an activated water molecule, and, finally, release of the product. Here we present the third species in this pathway, namely, the covalently bound intermediate. To more fully address the molecular changes that occur during catalysis, it will be necessary to solve the three-dimensional structure of the small subunit complexed with glutamine and with a tetrahedral mimic. This work is presently underway.

ACKNOWLEDGMENT

We thank Drs. W. W. Cleland, P. A. Tipton, and Ivan Rayment for helpful discussions. The insightful comments of K. M. Rayment and H. H. Rayment are also gratefully acknowledged.

REFERENCES

1. Thoden, J. B., Holden, H. M., Wesenberg, G., Raushel, F. M., and Rayment, I. (1997) *Biochemistry* 36, 6305–6316.
2. Thoden, J. B., Raushel, F. M., Benning, M. M., Rayment, I., and Holden, H. M. (1998) *Acta Crystallogr. D* (submitted for publication).
3. Zalkin, H. (1993) *Adv. Enzymol. Relat. Areas Mol. Biol.* 66, 203–309.
4. Mergeay, M., Gigot, D., Beckmann, J., Glansdorff, N., and Piérard, A. (1974) *Mol. Gen. Genet.* 133, 299–316.
5. Piette, J., Nyunoya, H., Lusty, C. J., Cunin, R., Weyens, G., Crabeel, M., Charlier, D., Glansdorff, N., and Piérard, A. (1984) *Proc. Natl. Acad. Sci. U.S.A.* 81, 4134–4138.
6. Tesmer, J. J. G., Klem, T. J., Deras, M. L., Davisson, V. J., and Smith, J. L. (1996) *Nat. Struct. Biol.* 3, 74–86.
7. Ollis, D. L., Cheah, E., Cygler, M., Dijkstra, B., Frolow, F., Franken, S. M., Harel, M., Remington, S. J., Silman, I., Schrag, J., Sussman, J. L., Verschueren, K. H. G., and Goldman, A. (1992) *Protein Eng.* 5, 197–211.
8. Khedouri, E., Anderson, P. M., and Meister, A. (1966) *Biochemistry* 5, 3552–3557.
9. Pinkus, L. M., and Meister, A. (1972) *J. Biol. Chem.* 247, 6119–6127.
10. Anderson, P. M., and Carlson, J. D. (1975) *Biochemistry* 14, 3688–3694.
11. Rubino, S. D., Nyunoya, H., and Lusty, C. J. (1986) *J. Biol. Chem.* 261, 11320–11327.
12. Miran, S. G., Chang, S. H., and Raushel, F. M. (1991) *Biochemistry* 30, 7901–7907.
13. Lusty, C. J. (1992) *FEBS Lett.* 314, 135–138.
14. Thoden, J. B., Raushel, F. M., Mareya, S., Tomchick, D., and Rayment, I. (1995) *Acta Crystallogr. D51*, 827–829.
15. Rossmann, M. G. (1972) *The Molecular Replacement Method*, Gordon and Breach, New York.
16. Navaza, J. (1994) *Acta Crystallogr. A50*, 157–163.
17. Tronrud, D. E., Ten Eyck, L. F., and Matthews, B. W. (1987) *Acta Crystallogr. A43*, 489–501.
18. Bricogne, G. (1976) *Acta Crystallogr. A32*, 832–847.
19. Ding, X., Rasmussen, B. F., Petsko, G. A., and Ringe, D. (1994) *Biochemistry* 33, 9285–9293.
20. Poland, B. W., Bruns, C., Fromm, H. J., and Honzatko, R. B. (1997) *J. Biol. Chem.* 272, 15200–15205.
21. Roux, B., and Walsh, C. T. (1993) *Biochemistry* 32, 3763–3768.

BI9807761